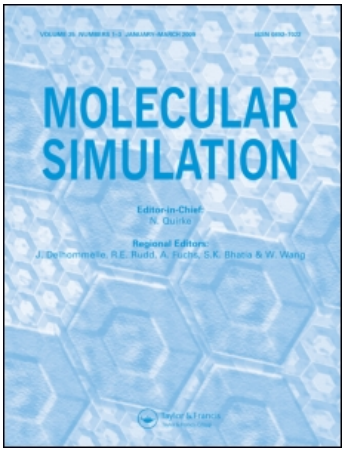

Molecular Simulation
Publication details, including instructions for authors and subscription information:
http://www.informaworld.com/smpp/title~content=t713644482

Comparative behavior of Pd and Ag deposition phenomenon on clean α-Al_2O_3 (001) surface—A first principle study

A. Chatterjee

To cite this Article Chatterjee, A.(2006) 'Comparative behavior of Pd and Ag deposition phenomenon on clean α-Al_2O_3 (001) surface—A first principle study', Molecular Simulation, 32: 2, 155 — 162
To link to this Article: DOI: 10.1080/08927020600688270
URL: http://dx.doi.org/10.1080/08927020600688270

Molecular Simulation, Vol. 32, No. 2, 15 February 2006, 155–162

Taylor & Francis
Taylor & Francis Group

Comparative behavior of Pd and Ag deposition phenomenon on clean α-Al_2O_3 (001) surface—A first principle study

A. CHATTERJEE*

Accelrys K.K., Nishishinbashi TS Building 11F, 3-3-1 Nishishinbashi, Minato-ku, Tokyo 105-0003, Japan

(Received December 2005; in final form March 2006)

The nature of bonding at the interface between deposited silver/palladium and clean Al-terminated (001) surface of α-Al_2O_3 has been investigated using a periodic *ab initio* method. Substantial inter-planar relaxations within the alumina were found at both the interfaces and the bulk. The periodic calculation with both Ag and Pd deposition shows that 10% of loading on alumina results maximum stability. Surface energy and work function calculations were performed to propose the stability for the metals on the studied surfaces. The deposited Ag forms a three-dimensional (3-D) cluster on top of the alumina surface. The Pd cluster formed on the alumina surface is two-dimensional (2-D) and is distorted to accommodate the Ag cluster in its domain. A further low index calculation can explain the reason for a higher stability of the membrane generated over alumina support with silver and palladium. The results are discussed in view of the existing experimental data and models of metal-oxide interface and a reason for the difference of activity of the metal interaction with alumina surface is postulated.

Keywords: Ag; Pd; Deposition; Clean α-Al_2O_3; (001) surface; Periodic *ab initio* method CASTEP

1. Introduction

The metal-ceramic based materials play a significant role in catalysis, photolysis and photooxidation reactions, electrocatalysis and gas sensors, etc. [1,2]. Aluminum oxide is one of the most widely used supports for catalytic purposes because of both its mechanical and thermal resistance. Experimental studies in this field are complicated by difficulties in preparing stoichiometric single crystal surfaces and by the sheer complexity of the bulk and surface oxide structures. It has been proved already that although, aluminum terminated surfaces may exist under vacuum [3,4] it is likely that surfaces exposed to oxygen and water have different terminations. The major experimental advances in terms of High-resolution electron-energy-loss spectroscopy (HREELS) [5] and micro-calorimetry [6] helped to understand the growth of high quality thin oxide films on conducting substrates. There is a specific interest to use metal cations on ceramic support for greater catalytic application.

Until recently, the understanding of bulk, surfaces and interfaces of oxides lagged far behind than that of semiconductors and metals [7]. This was partly because of the complexity of many oxide materials, which made them difficult to study with accurate theoretical methods and partly due to experimental difficulties. Density functional theory (DFT) methods have begun its venture in oxides somewhat later but progressed in a rapid manner. In the last couple of years, there have been considerable progresses in the area [8–13] of electronic and structural properties of mixed metal oxides using first principle DFT.

Verdozzi *et al.* [14,15] have performed a theoretical study of metals on sapphire, and identified two very different adsorption mechanisms, depending on the coverage. They have shown that while isolated adatoms are oxidized and bind strongly as ions, if coordinated to two or more other metal adatoms, the adsorbates are metallic, showing negligible charge transfer to the surface and relatively weak adsorption, mainly by polarization. They performed a local density approximation (LDA) calculation for structural and electronic properties of sapphire (0001), both clean and with d-metal over layers, which shows that the significant surface relaxations can penetrate to the third oxygen layer 5.2 Å below the surface. But the above-described method has its own limitation in terms of the definition of clean sapphire

*Corresponding author. Tel.: +81-03-3578-3861. Fax: +81-03-3578-3873. Email: achatterjee@accelrys.com

Molecular Simulation
ISSN 0892-7022 print/ISSN 1029-0435 online © 2006 Taylor & Francis
http://www.tandf.co.uk/journals
DOI: 10.1080/08927020600688270

surface itself. It has covered mainly the complex dynamics of water dissociation and related surface reactions. Kelber [16] and Chambers *et al.* [17,18] has shown that no clean sapphire surface exist except UHV. The clean sapphire surface is the normal terminated Alumina surface [19]. Jennison *et al.* [20] have extended the work of Chambers *et al.* [18] to a number of metals using first principle calculations and concluded that room-temperature process for creating metal-oxide interfaces discovered by Chambers on fully hydroxylated alumina, is a general phenomenon and could have many applications involving different metals. Kelber *et al.* [21] in one of their earlier paper had observed that the Cu growth on a partially hydroxylated α-Al_2O_3 (001) surface is dominated by two-dimensional (2-D) island formation, whereas, Cu growth on dehydroxylated surfaces is likely dominated by three-dimensional (3-D) island formation. Recently, we have used DFT to compare the activity of clean and hydroxylated (001) alpha alumina surface [22].

With this background, the current study aims firstly to rationalize the phenomenon of Ag and Pd deposition on α-Al_2O_3 and secondly to correlate the structure and property of Ag/Pd, deposited on the Al_2O_3 surface. We first studied the Ag/Pd loading from 1/3 to 1 ML over alumina (001) surface, to locate the optimum loading, where we assume 1/3 ML = 1 metal atom per surface oxygen atom for Al-terminated alumina surface. This has been followed by the calculation of low index Ag/Pd surfaces to monitor the role of surface packing on the activity. The interactions of low index Ag/Pd surfaces with the clean alumina surface are compared. The results as well propose the nature of the bonding of silver palladium with α-Al_2O_3.

2. Method and model

Ab initio total energy pseudopotential calculations were performed using Cambridge serial total energy package (CASTEP) and associated programs for symmetry analysis that has been described elsewhere [23,24]. In this code, the wave functions of valence electrons are expanded in a basis set of plane waves with kinetic energy smaller than a specified cutoff energy, E_{cut}. The presence of tightly bound core electrons is represented by non-local ultrasoft pseudopotentials [25]. CASTEP is a pseudopotential total energy code that employs Perdew and Zunger[26] parameterization of the exchange-correlation energy, super cells and special point integration over the Brillouin zone and a plane wave basis set for the expansion of wave functions. Becke-Perdew parameterization [27,28] of the exchange-correlation functional, which includes gradient correction (GGA), was employed. The pseudoptentials are constructed from the CASTEP database. The screening effect of core electrons is approximated by LDA, while the screening effect of valence electrons is taken care off by GGA. Reciprocal space integration over the Brilloin zone is approximated through a careful sampling at a finite number of k points using the Monkhorst-Pack scheme [29]. Here, we used symmetric 5 k-points in all calculations. The basis cut-off used is 380.0 eV. The energy tolerance is $5.0\,e^{-6}$ eV/atom, the force tolerance is 0.01 eV/Å, and the displacement tolerance is $5.0\,e^{-4}$ Å. To obtain equilibrium structures for a given set of lattice constants, ionic and electronic relaxations were performed using the adiabatic or "Born-Oppenheimer" approximation, where the electronic system is always in equilibrium with the ionic system. Relaxations were continued until the total energy had converged.

We have calculated the surface energy and work function for low index surfaces of Ag/Pd before and after deposition over α-Al_2O_3 to monitor the role of atomic packing on the activity of silver palladium.

The surface energy per surface atom is calculated as follows [30]:

$$\sigma = 1/2(E_{slab} - N_{atom}E_{bulk}).$$

where E_{slab} and E_{bulk} are the total energies for the slab (the cell containing N_{atom} atoms) and for bulk crystal (with a primitive cell), respectively. 1/2 is used as there are two surfaces in the slab model.

Work function is calculated as:

$$\varphi = E_{vac} - E_F$$

where E_{vac} and E_F are vacuum energy and Fermi energy, respectively. The vacuum energy is estimated by averaging the electrostatic potential over the middle plane of the vacuum layers.

Total energy calculations were performed on a supercell with periodic boundary conditions, which enables us to use a basis of plan waves. The supercell has the form of a rhombohedral prism, and in the stoichiometric slab it contains 30 atoms. This slab is exactly the thickness of one bulk unit cell of the corundum structure. Our surface calculations were performed on slabs repeated periodically in the z direction, with a vacuum space of thickness about equal to the slab. Figure 1 shows the structure with labeled atoms. The slab was hydroxylated on one surface. The opposite side of the slab was kept frozen at positions for the surface. This is necessary since a bulk-terminated surface is not stable due to its large surface dipole, which causes very large relaxations to occur [22] on this surface, which consists of 3 O-ions per unit cell and one Al-ion slightly above the O-plane. Periodically repeated slab super cells with eleven layers separated by nine layers of vacuum were used to model the Ag/Pd (1×1) surface.

3. Results and discussion

Our aim is to rationalize the structure of Ag/Pd over α-Al_2O_3 (001). We have performed the calculation for Al-terminated surface. So first we loaded Ag/Pd with increasing concentration from 1/3 to 1 ML and optimized the structure. The cell parameters were measured.

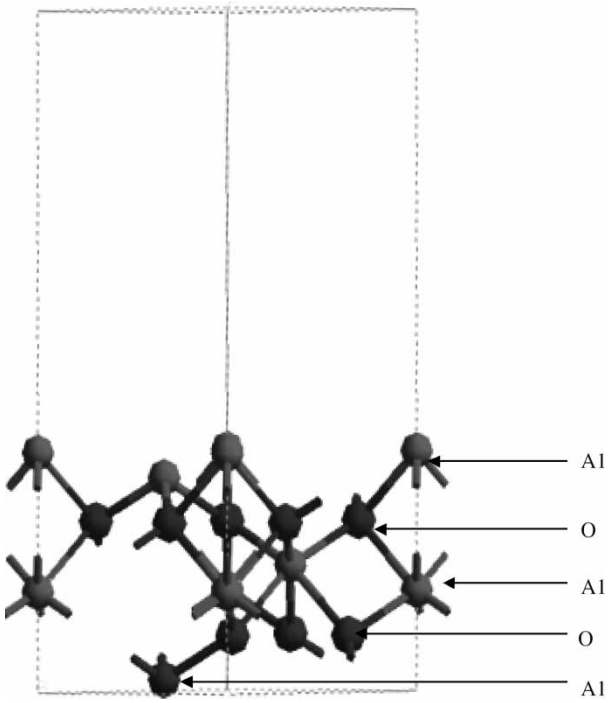

Figure 1. The periodic slab model representing α-Al_2O_3 with all the atoms labeled. The bottom two layers were fixed throughout the calculation.

The results showed in tables 1 and 2 represent the calculated metal surface binding after each Ag/Pd loading. We studied the various possible low index structures of silver palladium at it highest loading to monitor the effect of packing on activity. The surface energy and work function for the set of structures were shown in table 3. The effect of packing on the clean surface for both the metal deposition was compared.

3.1 Electronic structure of (001) surface of α-Al_2O_3 with and without Ag/Pd deposition using CASTEP

The (001) surface of α-Al_2O_3 has a layered structure, in which each oxygen plane in the bulk has an associated Al plane at a distance of 0.838 Å above and below, forming a stoichiometric triple layer. The most convenient unit cell is a rhombohedral prism comprising three such (001) oxygen planes separated by the associated pairs of Al

Table 1. Cell parameters for clean α-Al_2O_3, before and after incorporation of Ag/Pd with a reference to the results obtained by experiment for α-Al_2O_3.

Molecule	*a*	*b*	*c*	*α*	*β*	*γ*
Al-α-Al_2O_3	4.78	4.78	12.88	89.96	89.94	120.16
Experiment	4.75	4.75	12.99	90.00	90.00	120.00
Ag1-alumina	4.73	4.76	12.47	90.30	89.74	120.10
Pd1-alumina	4.66	4.63	12.60	90.23	88.55	120.27
Ag_2-alumina	4.81	4.81	12.52	90.11	89.88	120.32
Pd_2-alumina	4.71	4.73	12.47	89.90	90.15	120.43
Ag_3-alumina	4.91	4.88	12.69	87.31	91.34	120.44
Pd_3-alumina	4.82	4.75	12.32	88.36	90.49	120.45

Table 2. The total energy and binding energy as obtained for alumina lattices with Ag/Pd.

Periodic cell	*Total energy (eV)*	*Binding energy (eV)*	$E_{bind} - E_{coh}$ *(eV)*
α-Al_2O_3	−127.154		
Blank silver	−15.057		
Blank-Pd	−18.262		
1/3 ML of Ag-alumina	−149.122	−6.91	−5.35
1/3 ML of Pd-alumina	−155.029	−9.23	3.14
2/3 ML Ag-alumina	−165.827	−8.55	−3.41
2/3 ML Pd-alumina	−167.867	−9.12	2.76
1 ML Ag-alumina	−181.531	−9.20	−2.79
1 ML Pd-alumina	−188.537	−10.32	1.98
Test 1 with 2/3 Pd and 1/3 Ag	−196.241	−11.12	−2.98

planes. The oxygen planes are separated by 2.166 Å and form a hexagonal lattice with ABABAB... stacking. Their positions are slightly laterally distorted from ideal hexagonal sites. The Al atoms occupy two-thirds of the octahedral holes in the oxygen sub lattice, at the positions, which alternate between below and above the centers of these holes. The unoccupied octahedral holes are themselves stacked on a face centered cubic lattice, ABCABC. A C3v symmetry axis passes through each Al atom and through the centers of the unoccupied octahedral sites. The stoichiometric slab has two equivalent surfaces, which are terminated by an Al plane, as in figure 1. The termination defines the stoichiometric surface, because the slab as a whole is stoichiometric and has two equivalent surfaces.

We first optimized the aluminum lattice and the energy value is calculated using GGA (table 1). The results for Al-terminated surface are in match with the numbers generated by Wang *et al.* [31] and Batirev *et al.* [32]. It is observed that the planar relaxations are quite large, while the O ions and the Al ions remain essentially coplanar within ∼0.02 Å. The relaxation of surface Al is accompanied by a 9% reduction in the length of bond (1.687 Å) to the second layer oxygen, which is less than the experimental value of ∼4% [32]. The reduction is a natural consequence of the reduced coordination of surface Al. Coordination with the outermost O atoms also causes a shortening of bonds to interior Al neighbors (1.804 and 1.889 Å). These reductions result in part for the small lateral displacements within the O layer, which manifest them primarily as slight distortions and rotations of the triangles of O atoms below each surface Al. The predicted lateral displacement pattern qualitatively matches with the experimental values [31].

We loaded one Ag/Pd atom per surface oxygen atom or one Ag/Pd atom per three surface oxygen atoms (1/3 ML) and modeled until three Ag/Pd atoms saturating the surface oxygen resulting 1 ML of surface coverage, where three surface oxygens on the surface has three Ag/Pd. After each loading of Ag/Pd, the upper three layers of the structure including the Ag/Pd are optimized. The structure of alumina surface with two silvers (2/3 ML) two

Table 3. Surface energy (σ) and work function (φ) of Ag/Pd cluster calculated using GGA and LDA functional and compared with experiment.

	σ eV/atom				φ (eV)			
Cell	*GGA*	*LDA*	*Expt.*	*Al-Al_2O_3*	*GGA*	*LDA*	*Expt.*	*Al-Al_2O_3*
Ag (111)	0.357	0.530	0.55*	0.489	4.65	4.98	4.46†	5.73
Pd (111)	0.587	0.791	0.82	0.779	5.23	5.11	4.85	5.65
Ag (100)	0.432	0.633	0.88*	0.591	4.33	4.82	4.22†	5.41
Pd (111)	0.382	0.523	0.61	0.512	4.76	4.92	4.56	5.29
Ag (110)	0.649	0.952	1.18*	0.862	4.30	4.66	4.14†	5.17
Pd (110)	0.219	0.417	0.54	0.389	3.89	3.76	4.10	5.01

* Ref. [34]. † Ref. [35].

palladiums, three silvers (1 ML) and three palladiums before and after optimization is shown in figures 2–5 for clean Al-terminated alumina surface, respectively. The results of cell parameters as shown in table 1 depicts that with increase in Ag loading the cell parameters varies in an increasing order. The interesting feature is that with the increase on Ag loading there is a vertical quench observed compared to host alumina structure. The trend is reversed with palladium in *a* and *b* direction, where there is an expansion; where as there is an vertical quench in the *c* direction, but the cell expands back with increase in the loading of palladium. If the metal overlayer grows beyond 1 ML, the newly deposited atoms increase the coordination of and thereby stiffen the metal film interface, rendering it as bulk like; hence we did not perform anymore loading beyond 1 ML. This optimized silver sits just on top of the hexagonal whole comprised with aluminum and oxygen. In case of loading 2/3 ML silver, the optimized silver comes closer to each other at a distance of 1.87 Å, where as in case of 1 ML silver loading the optimized distance is 1.78 Å, for the Al-terminated surface. The results are as shown in figures 2 and 4, respectively. The silver atoms are connected to show the formation of the cluster. The average Ag–O distance is 2.43 Å, which is pretty much close with experimental values (2.45 Å) and better than that of Verdozzi *et al.* [14,15]. Silver atom is having a stronger bonding with α-Al_2O_3 surface that is largely caused by metal polarization. The aluminum and oxygen in clean relaxed α-Al_2O_3—are nearly coplanar (d12 = 0.04 Å), thereby neutralizing the surface polarity. The pattern changes significantly upon metal adsorption. The oxygen atom relaxes onwards by 0.3–0.5 Å and forces the aluminum ions to displace inward. This effect is much more pronounced at 1 ML loading, resulting in a favorable Ag–O bonding. Interestingly, the Al and O ions over the clean relaxed oxide surface are nearly coplanar. After the metal adsorption this changes dramatically. The oxygen atoms relax outwards by 0.2–0.5 Å. The large O–Al plane distance is observed for 1/3 ML loading. In the case of

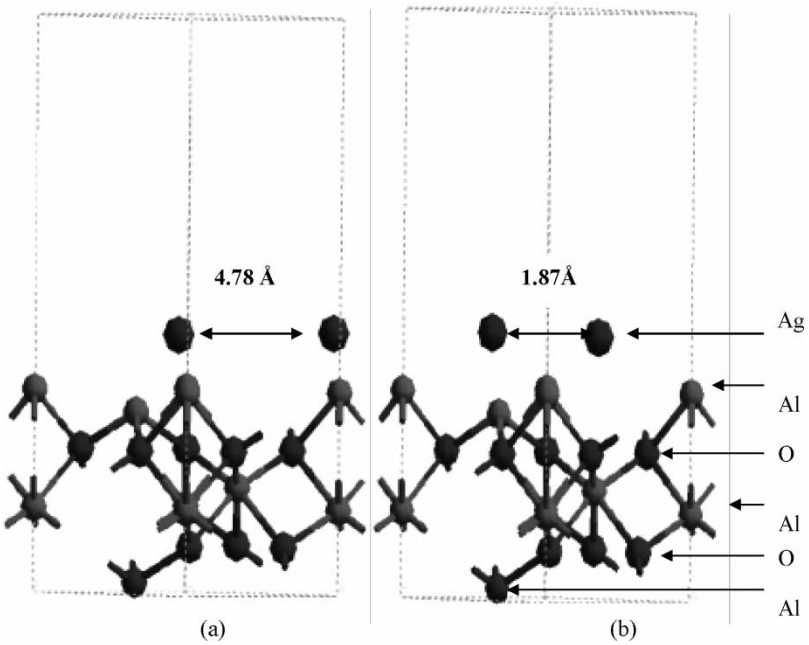

Figure 2. The structure of clean α-Al_2O_3 with 2/3 ML silver loading before and after optimization. The bottom two layers were fixed throughout the calculations.

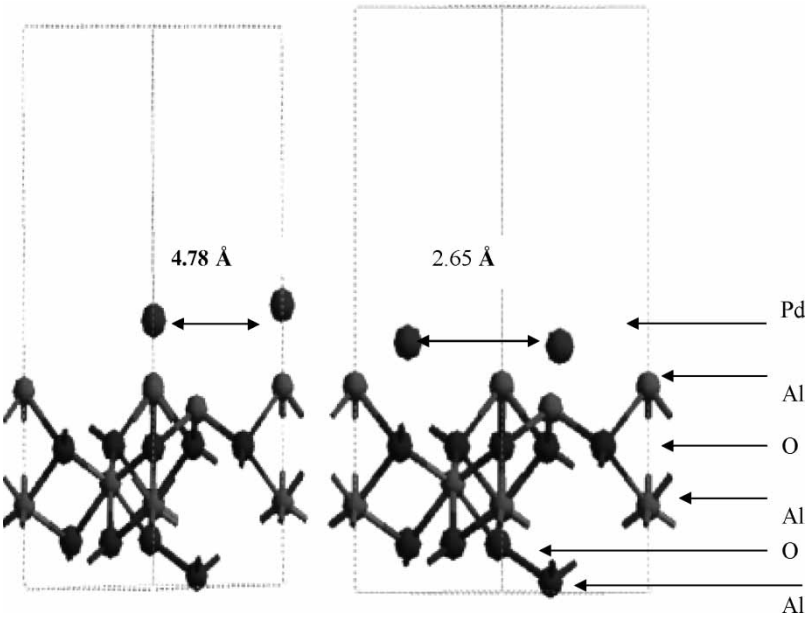

Figure 3. The structure of clean α-Al_2O_3 with 2/3 ML palladium loading before and after optimization. The bottom two layers were fixed throughout the calculations.

1/3 ML loading, the high relaxation may be due to the small size of Al cation and the repulsion of the ad ion-Ag. This further enhances the electrostatic potential of the adsorption site and the surface polarity decreases for 1 ML, as the layer over surface metal is neutral.

In case of optimized Pd, the trend is similar to that of silver, and the interatomic distances were very different from that of silver atoms. In case of 2/3 ML loading the optimized Pd go further to each other at a distance of 2.65 Å, where as in case of 1 ML loading the optimized distance is 2.56 Å, for the Al-terminated surface. The results are as well shown in figures 3 and 5, respectively. The Pd atoms looks much more relaxed on the surface and with increased loading. The Pd center prefers the edges of the alumina surface. The average Pd–O distance is 2.52 Å, the experimental support of which is not available though. The increase in Pd–Pd distance might be resulted from the repulsion of the Pd. This repulsion then forces the Ag to move out from polarized surface. The situation can be better understood from the surface with 1 ML of Pd

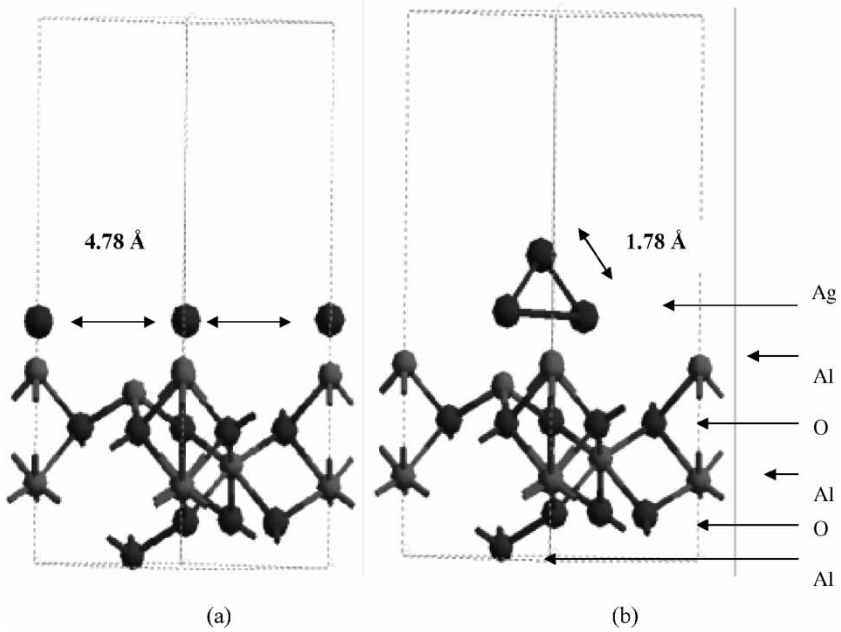

Figure 4. The structure of clean α-Al_2O_3 with 1 ML silver loading before and after optimization. The bottom two layers were fixed throughout the calculations.

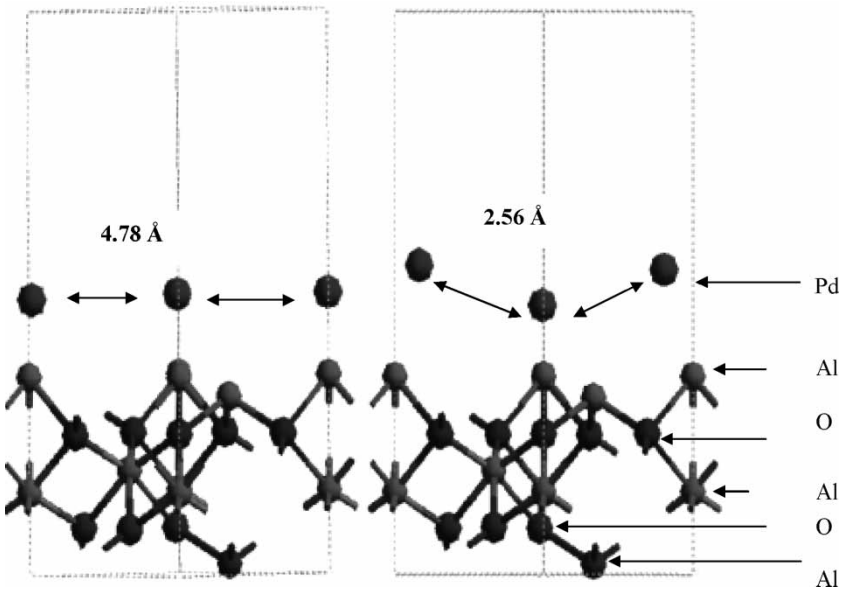

Figure 5. The structure of clean α-Al_2O_3 with 1 ML palladium loading before and after optimization. The bottom two layers were fixed throughout the calculations.

coverage. The above results from the geometric parameters show that the Pd stays much relaxed on the clean alumina surface compared to that of the silver. Now to rationalize the geometrical observations, we need to monitor the energetic of the systems.

3.2 The energetic of the interaction resulted due to deposition of Ag/Pd on clean alumina (001) surface

The total energy of the isolated system along with the system including adsorbed Ag and Pd; and their binding energy with each loading is studied and has been shown in table 2. The binding energy for metals over the alumina surface is calculated as the following:

$$E_{\text{binding}} = (NE_{\text{metal}} + E_{\text{Slab}} - E_{\text{total}})/N$$

where E_{binding} is the binding energy per metal atom binded to the alumina surface, E_{metal} is the energy of isolated metal atom, N is the number of metal atoms, E_{Slab} is the energy of the slab and E_{total} is the total energy of the metal adsorbed alumina system. Hence, the binding energy is defined as positive if the total energy decreases when the metal atom is brought from infinity and placed onto the surface.

For Al-terminated surface, the lattice with 1 ML of Ag/Pd shows highest binding energy in comparison to that with 2/3 ML Ag/Pd on surface and 1/3 ML of Ag/Pd loading on surface. This increase in binding energy with increasing coverage may be because of the ad atoms are polarized by the surface, and as a result they form non-negligible dipoles on the surface. The higher the coverage, the more pronounced the dipole–dipole repulsion among co-adsorbed silver atoms. In the last column, we report $E_{\text{bind}} - E_{\text{coh}}$ i.e. the difference between binding energy and the cohesive energy of the bulk Ag/Pd. A negative value suggests that the formation of a 3-D island of the Ag metal is more favorable than the formation of a single over layer on the oxide surface. This result of 2.35 eV is comparable to the cohesive energy computations of Philipsen and Baerends [33], who found a GGA fully relativistic energy for Ag of 2.37 eV as compared to an experimental value of 2.75 eV.

For the Pd system, it is observed that for 1 ML loading it shows the highest binding energy compared to other loadings. The steady increase in binding energy proposes stability. So individually these two metal ions are stable on the clean (001) alumina surface. Pd is more stable than the Ag for all the loading tried. Experimentally it is observed that Pd is more stable than Ag so far the mechanical stability is concern. It is observed that for Pd, the difference between binding energy and the cohesive energy of the bulk is a consistent positive value for all the loading. This shows that the Pd has a high chance to remain as a 2-D island on the clean alumina surface.

To test how a combination of Pd and Ag works I made a combination of 2/3 Pd and 1/3 Ag and optimized the structure with similar constrain, the structure after optimization is shown in figure 6. A very intriguing feature is observed. First, this composition makes the component more stable on clean (001) alumina surface. It is observed that this combination has a probability to stay as a 3-D island on the clean alumina surface. Now this can be explained in terms of the affinity of the individual components. To figure out the reason for this interesting behavior, I decided to perform a work function calculation with the metal clusters to find the role of packing of the clusters while binding with the alumina surface.

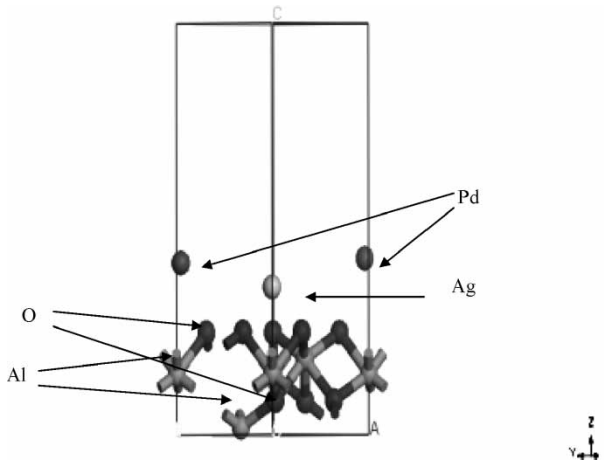

Figure 6. The structure of clean α-Al_2O_3 with 2/3 ML palladium and 1/3 ML of silver loading after optimization. The bottom two layers were fixed throughout the calculations.

3.3 Surface energy and work function calculations to monitor the effect of packing of Ag/Pd cluster on the clean alumina (001) surface

A set of calculations was performed with both the surfaces to rationalize the role of Ag/Pd packing with the surfaces. For both Ag and Pd three high symmetry low index surfaces, (111), (100) and (110) have been studied. The Miller planes are drawn to identify the structural orientation obtained after each low index packing. The Ag/Pd (1 × 1) surface systems are modeled using periodically repeated super cells; with eleven layers separated by nine layers of vacuum elongated slab. First, the surface energy per surface atom for each surfaces was calculated and then the work function for each surfaces were calculated (table 3). The surface energy and work function for the Ag surfaces are in close agreement with experiment [34,35]. In experiment, the surface energy and work function, was calculated by low-energy electron diffraction (LEED), high-energy ion scattering (HEIS), medium-energy ion scattering (MEIS) and Auger electron spectroscopy (AES) methods. Even I figured out that for the surface energy, the LDA results are in close agreement with the experimental values, whereas, for the work function GGA is a better performer. A totally opposite trend for surface energy per atom and the work function was found for Ag and Pd. For the surface energy, the values increases in the order of Ag (111) $<$ Ag (100) $<$ Ag (110); on the contrary in terms of work function, the order is Ag (110) $<$ Ag (100) $<$ Ag (111). A completely reverse trend is observed for Pd. So one can conclude that the activity of Ag/Pd is dependent with nature of their packing over alumina surface. The highest surface energy can also partially interpret their better activity, which projects the suitability of these surfaces for catalytic reactions on metal surfaces. Because of similar structural parameters, such as interlayer distance, surface roughness, both the (100) and (111) surfaces show similar characters. However, the properties of the Ag (110) surface differ from those of the (111) and (100) surfaces. Being on the top of the alumina, Ag (111) surface has a long-range interaction with the oxygen of alumina and a short-range interaction with the Al present in the top layer of alumina. The reverse trend for Pd give us a very good reason to believe that as the surface packing differs, the combination of Pd and Ag could result in a much more stable situation depending on the match of their packing. Hence, one can design their desired surface by comparing the activity of the surface following this convenient and simplistic simulation tool for pre-determined application issues.

4. Conclusion

This is the first systematic study to monitor the Ag/Pd deposition on α-Al_2O_3. I have monitored that for a 1 ML or 10% loading of Ag/Pd. Both Pd and Ag is stable over the surface with Pd has a higher stability, which validates the experimental result. I could further validate this stability by choosing a mixture composition with 2/3 Pd and 1/3 Ag to trace the stability of the mixtures. The presence of Pd give the structure an added stability whereas Ag act as the active ingredient for catalytic reaction. The silver forms a cluster over the Al layer of α-Al_2O_3 just on top of the hexagonal hole. The Ag/Pd bonding and activity are much more dependent on the structural relaxation of α-Al_2O_3. This brings us to look at the effect of their packing on the surfaces. The stability of a Pd/Ag combination can be validated through work function calculations. I found that the packing really changes the surface energy and hence the activity. Our final aim is to use the silver coated surface for some typical catalytic reaction. Both the surface energy and the work function results show that the atomic packing has direct correlation with activity. This will certainly influence the reactivity. I therefore, need to follow the catalytic reactions over the surface to probe the implications. Silver being a very good oxidation catalyst I am planning to look at some oxidation reactions over the best surfaces identified by this study.

References

[1] B.C. Gates. Supported metal clusters: synthesis, structure, and catalysis. *Chem. Rev.*, **95**, 511 (1995).
[2] R.M. Lambert, G. Pacchioni. *Chemisorptions and Reactivity on Supported Clusters and Thin Films: Towards an Understanding of Microscopic Processes in Catalysis*, Kluwer, Dordrecht, The Netherlands (1997).
[3] M. Gautier, G. Renaud, L.-P. Van, B. Villette, M. Pollak, N. Thormat, F. Jollet, J.P. Duraud. Alpha alumina surfaces—atomic and electronic structure. *J. Am. Ceram. Soc.*, **77**, 323 (1994).
[4] L. Stara, D. Zeze, V. Matolin, J. Pavluch, B. Gruzza. AES and EELS study of alumina model catalyst supports. *Appl. Surf. Sci.*, **115**, 46 (1997).
[5] V. Coustet, J. Jupille. High-resolution electron-energy-loss spectroscopy of isolated hydroxyl groups on α-Al_2O_3 (0001). *Surf. Sci.*, **307–309**, 1161 (1994).

[6] J.T. Stuckless, D.E. Starr, D.J. Bald, C.T. Cambell. Metal adsorption calorimetry and adhesion energies on clean single-crystal surfaces. *J. Chem. Phys.*, **107**, 5547 (1997).
[7] G.E. Brown, V.E. Henrich, W.H. Casey, D.L. Clark, C. Eggleston, A. Felmy, D.W. Goodman, M. Grätzel, G. Maciel, M.I. McCarthy, K.H. Nealson, D.A. Sverjensky, M.F. Toney, J.M. Zachara. Metal oxide surfaces and their interactions with aqueous solutions and microbial organisms. *Chem. Rev.*, **99**, 77 (1999).
[8] A. Asthagiri, D.S. Sholl. First principles study of Pt adhesion and growth on SrO- and TiO_2-terminated $SrTiO_3$ (100). *J. Chem. Phys.*, **116**, 9914 (2002).
[9] J.A. Rodriguez, S. Azad, L.Q. Wang, J. Garcia, A. Etxeberria. Gonzalez electronic and chemical properties of mixed-metal oxides: adsorption and reaction of NO on $SrTiO_3$ (100). *J. Chem. Phys.*, **118**, 6562 (2003).
[10] D.C. Sorescu, J.T. Yates, Jr. First principles calculations of the adsorption properties of CO and NO on the defective TiO_2 (110) surface. *J. Phys. Chem. B*, **106**, 6184 (2002).
[11] J.A. Snyder, D.R. Alfonso, J.E. Jaffe, Z. Lin, A.C. Hess, M. Gutowski. Periodic density functional LDA and GGA study of CO adsorption at the (001) surface of MgO. *J. Phys. Chem. B*, **104**, 4717 (2000).
[12] A. Asthagiri, D.S. Sholl. DFT study of Pt adsorption on low index $SrTiO_3$ surfaces: $SrTiO_3$(100), $SrTiO_3$(111) and $SrTiO_3$(110). *Surf. Sci.*, **581**, 66 (2005).
[13] J.A. Rodriguez, J.C. Hanson, S. Chaturvedi, A. Maiti, J.L. Brito. Studies on the behavior of mixed-metal oxides: structural, electronic, and chemical properties of β-$FeMoO_4$. *J. Phys. Chem. B*, **104**, 8145 (2000).
[14] C. Verdozzi, D.R. Jennison, P.A. Schulz, M.P. Sears. *Phys. Rev. Lett.*, **82**, 799 (1999).
[15] J.M. Wittbrodt, W.L. Hase, H.B. Schlegel. *Ab Initio* study of the interaction of water with cluster models of the aluminum terminated (0001) α-aAluminum oxide surface. *J. Phys. Chem. B*, **102**, 6539 (1998).
[16] M. Gazra, N.P. Magtoto, J.A. Kelber. Characterization of oxidized Ni_3Al (110) and interaction of the oxide film with water vapor. *Surf. Sci.*, **519**, 259 (2002).
[17] P. Liu, T. Kendelewicz, G.F. Brown, Jr., E.J. Nelson, S.A. Chambers. Fe_2O_3 (0001) surfaces: synchrotron X-ray photoemission studies and thermodynamic calculations. *Surf. Sci.*, **417**, 53 (1998).
[18] S.A. Chambers, T. Droubey, D.R. Jennison, T.R. Matsson. Laminar growth of ultra thin metal films on metal oxides: Co on hydroxylated α-Al_2O_3 (0001). *Science*, **297**, 827 (2002).
[19] P. Guenard, G. Renaud, A. Barbier, M. Gautier-Soyer. Determination of the alpha-Al_2O_3 (0001) surface relaxation and termination by measurements of crystal truncation rods. *Surf. Rev. Lett.*, **5**, 321 (1998).
[20] D.R. Jennison, T.R. Mattsson. Atomic understanding of strong nanometer-thin metal/alumina interfaces. *Surf. Sci.*, **544**, L689 (2003).
[21] J.A. Kelber, C. Niu, K. Shepherd, D.R. Jennison, A. Bogicevic. Copper wetting of α-Al_2O_3 (0001): theory and experiment. *Surf. Sci.*, **446**, 76 (2000).
[22] A. Chatterjee, S. Niwa, F. Mizukami. Structure and property correlation for Ag deposition on α-Al_2O_3—a first principle study. *J. Mol. Graphics Model.*, **23**, 447 (2005).
[23] M.P. Teter, M.C. Payne, D.C. Allen. Solution of Schrödinger's equation for large systems. *Phys. Rev. B*, **40**, 12255 (1989).
[24] M.C. Payne, M.P. Teter, D.C. Allen, T.A. Arias, J.D. Johannopoulos. Iterative minimization techniques for ab initio total-energy calculations—molecular dynamics and conjugate gradients. *Rev. Modern. Phys.*, **64**, 1045 (1992).
[25] D. Vanderbilt. Soft self-consistent pseudopotentials in a generalized eigenvalue formalism. *Phys. Rev. B*, **41**, 7892 (1990).
[26] J. Perdew, A. Zunger. Self-interaction correction to density-functional approximations for many-electron systems. *Phys. Rev. B*, **23**, 5048 (1981).
[27] J.P. Perdew. Density-functional approximation for the correlation energy of the inhomogeneous electron gas. *Phys. Rev. B*, **33**, 8822 (1986).
[28] A.D. Becke. Density functional exchange energy approximation with correct asymptotic behavior. *Phys. Rev. A*, **38**, 3098 (1988).
[29] H.J. Monkhorst, J.D. Pack. Special points for Brillouin-zone integrations. *Phys. Rev. B*, **13**, 5188 (1976).
[30] W. Wang, K. Fan, J. Deng. Structural and electronic properties of silver surfaces: *ab initio* pseudopotential density functional study. *Surf. Sci.*, **490**, 125 (2001).
[31] Y. Wang, X.-G. Wang, A. Chaka, M Scheffer. The Hematite (alpha—Fe_2O_3) (0001) surface: evidence for domains of distinct chemistry. *Phys. Rev. Lett.*, **81**, 1038 (2000).
[32] I.G. Batirev, A. Alavi, M.W. Finnis, T. Deutsch. First-principles calculations of the ideal cleavage energy of bulk niobium (111)/alpha-alumina (0001) interfaces. *Phys. Rev. Lett.*, **82**, 1510 (1999).
[33] P.H.T. Philipsen, E. Baerends. Relativistic calculations to assess the ability of the generalized gradient approximation to reproduce trends in cohesive properties of solids. *Phys. Rev. B*, **61**, 1773 (2000).
[34] M. Chelvayohan, C.H.B. Mee. Work function measurements on (110), (100) and (111) surfaces of silver. *J. Phys. C: Solid State Phys.*, **15**, 2305 (1982).
[35] L. Vattuone, M. Rocca, C. Boragno, U. Valbusa. Initial sticking coefficient of O_2 on Ag (110). *J. Chem. Phys.*, **101**, 713 (1994).